

Profile properties of deteriorating columnar ice:  
Implications for modelling ice-cover flexural failure<sup>1</sup>

M.N. Demuth and T.D. Prowse

National Hydrology Research Institute  
Environment Canada  
11 Innovation Blvd.  
Saskatoon, Canada  
S7N 3H5

ABSTRACT

Flexural failure is generally recognized to be a dominant process characterizing river-ice break-up. Estimating the resistance of an ice cover to flexural deformation requires knowing its bending properties. This information is also needed to estimate the bearing capacity of floating ice covers. In most past studies, analyses of flexural failure have assumed the ice to be a vertically isotropic material. River-ice covers have a highly-variable structure which can significantly affect the distribution of the strength and strain modulus in the vertical profile plane. This paper discusses morphologic, thermal and mechanical parameters affecting the resultant distribution of stress for a deteriorating fresh-water ice cover subjected to bending. The development of two contrasting ice-cover deterioration states, at depth and at the surface, is generated by a numerical ice deterioration model. Composite plate-bending theory is applied to illustrate the effects of temperature and porosity variations on the bending stress profile. The inaccuracies inherent in homogeneous bending theory are illustrated.

KEY WORDS

|               |                      |
|---------------|----------------------|
| Bending       | Ice Strength         |
| Break-up      | Melt                 |
| Deterioration | Numerical Model      |
| Elasticity    | River-Ice            |
| Failure       | Short-Wave Radiation |
| Heat Transfer | Stress               |

<sup>1</sup> NHRI Contribution Series Number CS-91051  
ph. 306 975 5754

## INTRODUCTION

Knowledge of ice failure processes is a prerequisite to accurate modelling of river-ice break-up. While it has been generally established that flexural failure is a dominant break-up mechanism (e.g., Billfalk, 1982; Beltaos, 1990; Prowse and Demuth, 1989; Demuth and Prowse, 1990), most analyses have assumed the ice sheet to be vertically homogeneous. River-ice sheets are, however, highly complex in their physical and thermal characteristics. Moreover, parameters important to the analysis of ice failure, such as ice strength and strain modulus, are largely dependent on these same ice characteristics. Hence, results and conclusions concerning break-up processes based on "homogeneous material" assumptions must be evaluated with caution.

Knowledge of the true stress distribution in bending, derived from the influence of vertical inhomogeneity, allows a more accurate investigation of conditions necessary for failure.

## PROFILE CHARACTERISTICS OF FRESH-WATER ICE

### Basic Morphology of River Ice

The physical and thermal characteristics of an ice cover at the time of break-up depend on the hydraulic and meteorologic conditions that led to ice formation, growth and decay. The following provides a generalized view of the complexities in cover characteristics, particularly those that can vary in the vertical and are important in controlling the stresses associated with flexural deformation.

In the simplest case of calm flow or late-freezing polynyas, static ice formation dominates and the surface is comprised of columnar-grained ice. More commonly, however, river ice forms by dynamic processes in which various evolutionary stages of frazil ice lead to a surface varying from a thin veneer to a multi-layered freeze-up jam many metres thick.

The grain geometry and thickness of this initial layer affect, respectively, the subsequent alignment of grains and the overall rate of secondary ice growth; the latter in turn controlling grain diameter, bubble size and density, and impurity content.

Irrespective of initial grain diameter, the vertical growth of static ice is usually characterized by a progression with depth to larger diameter grains. One exception is where the accumulation of frazil beneath a cover can accelerate ice growth and also complicate the grain structure. A somewhat analogous situation can develop at the surface of the ice sheet where surface snow is flooded and refreezes into a superimposed snow-ice formation.

Hence, at the end of the growth period, the vertical structure of river ice can be highly complex. Such complexity can be further increased during the pre-break-up melt phase. The convective and radiative heat fluxes preceding break-up determine the range in temperatures and the shape of the vertical temperature profile through the ice sheet that will prevail at the time of ice failure. In cases where the heat fluxes produce a 0°C state within or throughout an ice sheet, additional inputs of short-wave radiation can produce significant structural changes through the development of melt pores. Radiation-induced melt is usually first evident at grain boundaries but what starts as a thin film of inter-granular water can develop into large melt pockets and channels. The size and concentration of these decrease with depth according to the rate of radiation attenuation; the rate being most rapid in granular ice and less so in columnar ice.

#### Influence of Cover Characteristics on Strength and Strain Modulus

Many studies have focused on quantifying homogeneous samples in which the value of a particular parameter does not vary. The following summarizes trends observed in existing data sets for fresh-water ice.

### *Ice Type*

In general granular ice, which includes congealed frazil ice (S4) and the superimposed snow ice (T1), is the strongest. The strength of columnar-grained ice varies depending whether the loading direction is parallel or perpendicular to the columnar axis; the former is strongest and closely corresponds to granular ice. Other potential effects involve variations in the crystallographic orientation of columnar ice forms. S1 ice, having a vertical c-axis orientation, is stronger in both tension and compression than S2 ice whose c-axes are horizontal (e.g., Carter and Michel, 1971; Michel and Drouin, 1971). Random or highly directional c-axis alignments can also effect strength (e.g., Weeks and Gow, 1978). Various ice types exhibit different theoretical strain modulus values, with granular ice being, in general more compliant than columnar forms (e.g., Michel, 1978).

### *Grain Size*

In general finer grain sizes lead to an increase in strength (e.g. Cole, 1986; Jones and Chew, 1983). This effect is particularly apparent in data describing ice subjected to tensile stresses (e.g., Michel 1978).

### *Thermal - Temperature*

Ice strength is strongly controlled by temperature, particularly in compression. Strength increases with falling temperature. Data for ice in tension indicate that temperature plays a smaller role (e.g., Michel, 1978). The effect of temperature on ice strain modulus is similar in so far as warm ice is more compliant than cold ice.

### *Porosity*

Ice porosity is a particularly important modifier of strength and strain modulus, as evidenced by data from physical measurements and theoretical considerations. Porosity is the ratio of void space to the solid ice volume. In natural fresh-water ice, it is

derived from air bubbles and/or melt-water.

Most work to date has ignored the potential effects of air porosity. This is primarily due to the difficulty of measuring air porosity (e.g., Tabata, 1958). Observations by Gow and Langston (1977), indicate that in the bubbliest ice found in typical lakes, the air planar porosity is unlikely to be above  $\approx 0.03-0.04$ . For spherical geometry this translates to a volumetric porosity of  $0.038-0.06$  - not insignificant.

Liquid pore-space induces a marked reduction in the strength and strain modulus of saline ice (e.g., Mellor, 1983 and Tabata, 1958). There is a paucity of data, however, for  $0^{\circ}\text{C}$  porous ice. Recently, Prowse *et al.* (1990) measured the reduction of strength associated with the formation of melt pores due to the absorption of solar radiation for  $0^{\circ}\text{C}$  fresh-water columnar ice. They estimate a four-fold reduction in the compressive strength of ice having attained a melt-fraction porosity of 0.1 compared to the value for intact  $0^{\circ}\text{C}$  ice.

#### *Mechanical Profile Parameters*

In quantifying ice flexural processes, it should be recognized that important mechanical profile parameters such as stress mode (tensile, compressive) and stress rate vary throughout the vertical plane in a specimen subject to bending. The rate and stress-mode dependence of ice strength and strain modulus have been well documented (e.g., Gold, 1977; Sinha, 1981a; 1981b). The uniaxial compressive strength and strain modulus for ice increases with increasing strain rate. Ice is generally weaker in tension than in compression, but this too varies with strain rate.

Thus, there are numerous cover characteristics and mechanical profile parameters that can affect the strength and strain modulus of river ice. For simplicity, the following sections focus on

only two characteristics, temperature and melt porosity, to demonstrate the importance of such natural sources of heterogeneity when conducting bending failure analysis. Composite bending theory is applied to two pre-break-up deterioration cases; one in which structural deterioration evolves at depth, the other dominating the surface. For simplicity, a static ice cover, comprised entirely of S2 columnar-grained ice is assumed.

## ANALYSIS AND RESULTS

### Modelling Ice-Deterioration

Ice-cover deterioration involves the warming and structural deterioration of the ice matrix by convective and radiative heat fluxes. Ashton (1981) developed a method for predicting changes in the strength of columnar-grained ice based on a first-order deterioration model (herein referred to as ROT) which uses generally accepted algorithms for calculating the convective and radiative heat-transfer components from basic meteorologic data. Specifically, the sensible heat transfer ( $Q_h$ ) is calculated using bulk heat transfer coefficients, wind speed and air temperature ( $T_a$ ). The latent heat term ( $Q_e$ ) is estimated from the Bowen ratio method. The long-wave exchange ( $Q_{lw}$ ) is estimated using the Brunt equation which considers the effects of cloud and humidity (R.H.). The short-wave (solar) ( $Q_s$ ) component is calculated as a function of solar zenith-, declination- and hour angles, vapour pressure and cloud fraction. The short-wave radiation penetrating the surface ( $Q_{sp}$ ) is determined using a bulk coefficient representing albedo ( $\alpha$ ). The transmission and attenuation of short-wave radiation in the ice is modelled according to an exponential extinction function whose extinction coefficient is depth-dependent. Heat conduction, inter-granular melt and freeze-back are modelled using an explicit finite-difference algorithm.

### Sample Case Studies

Two energy-balance scenarios which represent i) cold - high radiation and ii) warm - high radiation conditions are presented.

A modified version of ROT is used to model ice-cover deterioration (warming and porosity development) and the output employed to predict changes in the stress-distribution of such ice covers subjected to bending.

*Case I: Deterioration at Depth Below Cold Layer*

This case illustrates an ice cover developing structural deterioration (porosity development) at depth, even though near-surface strata are intact and well below  $0^{\circ}\text{C}$  (Figures 1, 3). Such conditions can exist when net  $Q_{lw}$ ,  $Q_h$  and  $Q_e$  are negative but net  $Q_s$  is very high. The result is a near-surface heat deficit produced by the strong ice-air heat flux (i.e.,  $Q_{lw} + Q_h + Q_e$ ) which is gradually offset with depth by the attenuating  $Q_{sp}$ . The magnitude of this offset at any point in the vertical depends on the relative rate of heat conduction to the cooling surface and the rate to which it is warmed by  $Q_{sp}$ . Hence, further down the profile the ice temperature is raised to the melting point, while further along, enough energy exists to cause inter-granular melt.

*Case II: Surface Deterioration*

The second case is where the combined heat loss from  $Q_{lw}$ ,  $Q_h$  and  $Q_e$  is less than that input by  $Q_s$  even at the surface. The end result is an ice-cover that is gradually brought to a  $0^{\circ}\text{C}$  isothermal state. Once this occurs,  $Q_{sp}$  is able to produce structural decay throughout the profile following the exponential attenuation with depth (Figures 2, 3). Near-surface refreezing occurs at night when  $Q_s$  is zero and the long-wave and convective terms become negative.

Bending Theory for Vertically-Anisotropic Ice

The distribution of stress about the bending plane, for a vertically-anisotropic plate, depends on the distribution of strain modulus by controlling the position of the neutral plane and the magnitude of the flexural rigidity. The neutral plane is determined by balancing what effectively is the resistance to

deformation in the tensile and compressive zones such that:

$$[1] \quad Z_n = t - \frac{\int_0^t E'(z) (t - z) dz}{\int_0^t E'(z) dz}$$

where  $Z_n$  is the distance to the neutral plane from the ice surface,  $t$  is the ice thickness,  $E'(z)$  is the distribution of effective strain modulus along the vertical bending plane and  $z$  is the vertical co-ordinate axis. For  $E'(z) = \text{constant}$ ,  $Z_n = t/2$ . In equation [1],  $E'$  is used as opposed to  $E$ , the theoretical Young's modulus, because usually, under test conditions or in nature, some degree of delayed elastic strain effectively reduces ice compliance. Using effective values then allows the realistic application of elastic theory.

The composite-plate flexural rigidity  $D$  is determined from:

$$[2] \quad D = \int_0^t \frac{E'(z) (z - Z_n)^2}{1 - \nu^2} dz$$

where  $\nu$  is the Poisson ratio. For  $E'(z) = \text{constant}$ ,  $D' = E't^3/(12(1-\nu^2))$ . The normal bending stress  $\sigma_x(z)$  is then determined from:

$$[3] \quad \sigma_x(z) = \frac{M}{(1 - \nu^2) D} (z - Z_n) E'(z)$$

where  $M$  is the applied moment.

To describe the stress distribution along the bending plane,  $E'(z)$  must be determined as a function of ice temperature ( $T$ ) and liquid fraction porosity ( $\phi_1$ ).

Although many data describing the variation of  $E'$  with temperature and porosity exist for cold fresh-water ice and saline ice, there



is a lack of data for 0°C porous fresh-water ice. A reasonable approximation for  $E' = f(\phi_1)$  would be to use a general relationship for  $E'$  based on flexural data from a variety of large-scale *in-situ* and small-scale laboratory tests of porous saline ice. Data by Vaudrey (1977), reported by Cox and Weeks (1986), describe the variation of  $E'$  with porosity using:

$$[4] \quad \frac{E'}{E'_0} = 1 - A \sqrt{\phi_1}$$

where  $E'_0$  represents the value at  $\phi_1 = 0$  and  $A$  is an empirical constant. A reasonable fit is achieved for  $A = 2.5966$  and  $E'_0 = 5.31$  GPa. This latter value appears plausible for  $\phi_1 = 0$  and  $T = 0^\circ\text{C}$ , for the trends in data describing  $E' = f(T)$  for columnar-grained non-saline ice (e.g., Traetteberg *et al.*, 1975; Sinha, 1978). These data result in the following relationship:

$$[5] \quad E' = 5.31[1 - 0.0228 T] \quad (\text{GPa})$$

where  $T$  is in  $^\circ\text{C}$ . For elastic behaviour,  $E'$  in tension and compression are approximately equal (e.g., Mellor, 1983).

Profiles of ice temperature and porosity were extracted for three instances: Case I Hour 02 (I02); Case I Hour 64 (I64) and Case II Hour 14 (II14), each characterizing a contrasting thermal/structural regime (Figure 4). Equations [4,5] were used to determine  $E'$  at depth  $z$ .  $\sigma_x(z)$ , per unit  $M$ , is determined for bottom in tension (tension - positive) using equations [1,2,3] and  $\nu = 0.3^1$  (Mellor, 1983).

---

<sup>1</sup>  $\nu$  varies with porosity such that it can influence the elastic moduli (e.g.,  $E$  and the bulk modulus  $K$ ) used in applying elastic continuum theory to porous materials. For this analysis, it is assumed that porosity is derived entirely from melt pores. Since  $K$  of water and ice are not significantly different, the effect of water-filled melt pores on  $\nu$  would then be controlled primarily by the corresponding variation of  $E'$ .

## RESULTS AND DISCUSSION

### Case I

Profile I02 (Figure 4) represents a completely intact ice-cover exhibiting a modest temperature gradient, steeper near the surface where the surface temperature is approximately  $-12^{\circ}\text{C}$ , and gradually rising to  $0^{\circ}\text{C}$  at the ice-water interface. The temperature effect on  $E'$  and  $\sigma_x$  is clearly evident. The stress distribution varies significantly from that produced under a simple homogeneity assumption (i.e.,  $E'(z) = \text{constant}$ ). Effects of temperature on stress profiles can be much more extreme than those shown; Kerr and Palmer (1972), for example, present a more detailed treatment of such effects.

Profile I64 depicts a small near-surface thermal gradient with gradually increasing structural deterioration with depth to  $\phi_1 \approx 0.045$  near the ice-water interface. The difference in stresses (homogeneous versus anisotropic) is strongest below the neutral axis where the ice is generally more compliant. For comparison "Positive"<sup>2</sup> T represents a "warm content" and can be converted to a melt porosity by  $\phi_1 = \Delta T C_p / \lambda$ ; where  $C_p$  is the specific heat and  $\lambda$  is the latent heat of fusion for ice (see lower ordinate-Figure 4). A variation of negative T in the intact region of profile I02 has a smaller effect than an even smaller variation of porosity ("positive" T) in the deteriorating region of profile I64. The maximum tensile stress is not at the outer-most tensile fibre while the overall maximum stress is compressive.

### Case II

Profile I114 shows structural deterioration dominating the surface strata with  $\phi_1$  reaching 0.12 near the surface. The porosity gradient is steep near the surface becoming somewhat uniform and near zero throughout the remainder of the profile. The homogeneous and anisotropic stress profiles again vary but now

---

<sup>2</sup> A result of the finite-difference scheme employed.

most noticeably above the neutral axis in the zone of significant structural deterioration. The maximum stress in compression occurs in from the surface boundary and the overall maximum stress is tensile.

#### DISCUSSION AND CONCLUSIONS

This paper has shown that variations in various morphologic, thermal and mechanical ice parameters can affect vertical stress profiles compared with those assumed using homogeneous plate-bending theory. Specifically, for ice covers exhibiting significant temperature gradients or melt-induced porosity, homogeneous theory distorts fibre stresses throughout the profile. This distortion is proportional to the distribution and magnitude of temperatures and porosity, with porosity, in general, having a greater effect. The position of the maximum stress may be in the interior of the plate as opposed to the outer surfaces as assumed by homogeneous theory. The maximum stress may be compressive, depending on whether the plate is deflected upward or downward, and whether compliance reduction is more marked in zones below or above the neutral plane. Such considerations have important implications for modelling the forces necessary to precipitate bending failure in pre-break-up ice covers.

A myriad of meteorologic and ice-cover parameters can affect the distribution and magnitude of warming and structural deterioration in an ice cover. Hence, numerous deterioration scenarios are possible under natural conditions. As illustrated, structural deterioration at depth is one such process not acknowledged or even possible to quantify using conventional approaches to forecasting break-up (e.g., when surrogate heat indices such as melting degree-days are employed).

Although the analytical portions of this paper have focused on the effects of temperature and porosity, the methodology could be extended to include the effects of other profile parameters. This

would also require that suitable physical or empirical relationships describing modifications to  $E'$  could be generated.

#### ACKNOWLEDGEMENTS

The authors thank Dr G.D. Ashton for access to the source code for the numerical ice deterioration model, and Mr B. Reid of NHRI for help in data reduction and illustrations.

#### LITERATURE CITED

- ASHTON, G.D. 1981: Deterioration of floating ice covers. *Journal of Energy Resources Technology*, 107(2), 177-182.
- BELTAOS, S. 1990: Fracture and breakup of river ice cover. *Canadian Journal of Civil Engineering*, 17(2), 173-183.
- BILLFALK, L. 1982: Break-up of solid ice covers due to rapid water level variations. CRREL Report 82-3, 17p.
- CARTER, D. and MICHEL, B. 1971: Lois et mécanismes de l'apparant fracture fragile de la glace de rivière et de lac. Département de Génie Civil, Université Laval, Québec, Canada, Report No.S-22.
- COLE, D.M. 1986: Effect of grain size on the internal fracturing of polycrystalline ice. CRREL Report 86-5, 71p.
- DEMUTH, M.N. and PROWSE, T.D. 1990: A physical model of ice overthrust during the break-up of intact river-ice covers. *Northern Hydrology: Selected Perspectives, Proceedings of the 1990 Northern Hydrology Symposium*, Saskatoon, Canada, 57-73.
- COX, G.N.F. and WEEKS, W.F. 1986: On the profile properties of undeformed first-year sea ice. CRREL Special Report 86-30, 2<sup>nd</sup> Workshop on Ice Penetration, Monterey, U.S.A., 257-330.
- GOLD, L.W. 1977: Engineering properties of fresh-water ice. *J. Glaciology*, 19(81), 197-212.
- GOW A.J. and LANGSTON, D.L. 1977: Growth history of lake ice in relation to its stratigraphic, crystalline and mechanical structure. CRREL Report 77-1, 29p.
- JONES, S.J. and CHEW, H.A.M. 1983: Effect of sample and grain size on the compressive strength of ice. *Annals of Glaciology*, (4), 129-132.
- KERR, A.D. and PALMER, W.T. 1972: The deformations and stresses in floating ice plates. *Acta Mechanica* 15, 57-72.

- MELLOR, M. 1983: Mechanical behaviour of sea ice. CRREL Monograph 83-1, 102p.
- MICHEL, B. 1978: Ice Mechanics. Les Presses de l'Université Laval, Québec, Canada, 499p.
- MICHEL, B and DROUIN, M. 1971: Les propriétés mécaniques à l'impact de la glace du Saint-Laurent. Département de Génie Civil, Université Laval, Québec, Canada, Report No.T-19.
- PROWSE, T.D. and DEMUTH, M.N. 1989: Failure modes observed during river-ice breakup. Proceedings of the 46<sup>th</sup> Eastern Snow Conference, Québec, Canada, 237-241.
- PROWSE, T.D., DEMUTH, M.N. and CHEW, H.A.M. 1990: The deterioration of fresh-water ice due to radiation decay. J. Hydraulic Research, 28(6), 685-697.
- SINHA, N.K. 1978: Short-term rheology of polycrystalline ice. J. Glaciology, 21(85), 457-472.
- SINHA, N.K. 1981a: Rate sensitivity of compressive strength of columnar-grained ice. Experimental Mechanics, 18(12), 464-470.
- SINHA, N.K. 1981b: Constant stress rate deformation modulus of ice. POAC, Québec, Canada, V.1, 216-224.
- TABATA, T. 1958: Studies on the visco-elastic properties of sea ice. In Arctic Sea Ice, U.S. National Academy of Sciences, National Research Council, Publication 598, 139-147.
- TRAETTEBERG, A., GOLD, L.W. and FREDERKING, R. 1975: The strain rate and temperature dependence of Young's modulus of ice. International Symposium on Ice Problems, IAHR, Hanover, U.S.A., 479-486.
- VAUDREY, K.D. 1977: Ice engineering: Study of related properties of floating sea-ice sheets and summary of elastic and viscoelastic analysis. U.S. Naval Civil Engineering Laboratory, Technical Report R860, 79p.
- WEEKS, W.F. and GOW, A.J. 1978: Crystal alignments in the fast ice of arctic alaska. J. Geophysical Research 85(C2), 1137-1146.

FIGURE 1 Schematic of heat-flux terms (after Ashton, 1981) and the meteorological conditions generated by ROT for CASE I-Deterioration at Depth.

FIGURE 2 Schematic of heat-flux terms and meteorological conditions generated by ROT for CASE II-Surface Deterioration.

FIGURE 3 Time series of warming, nocturnal cooling and structural deterioration for three consecutive days under the influence of the meteorological conditions described in Figures 1, 2.

FIGURE 4 Extracted profiles of ice temperature, porosity, the resulting effective strain modulus distribution,  $E'(z)$  and the corresponding bending-stress distribution.

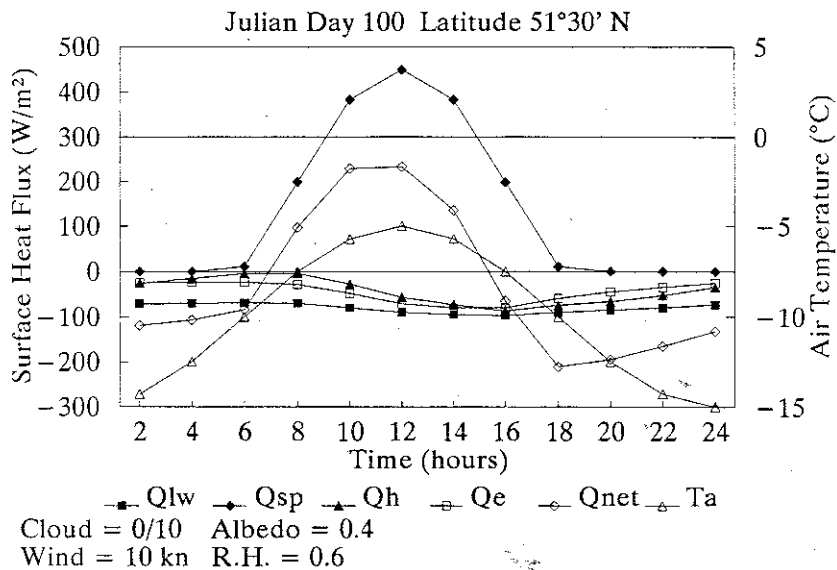
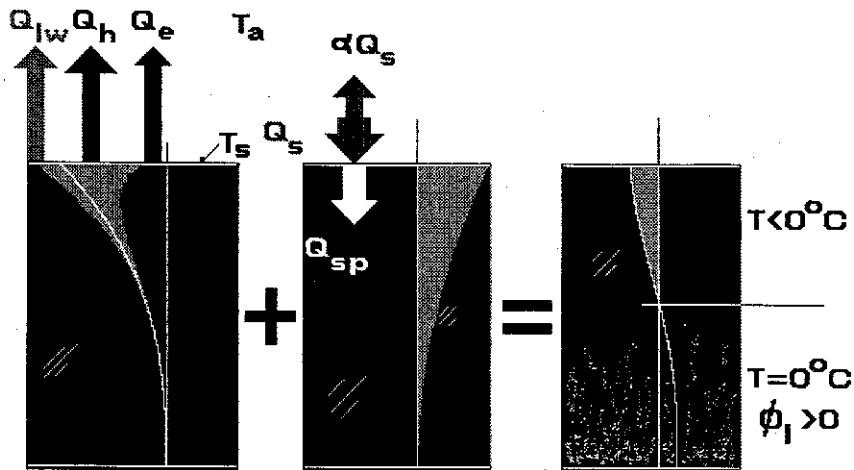


FIGURE 1 Schematic of heat-flux terms (after Ashton, 1981) and the meteorological conditions generated by ROT for CASE I-Deterioration at Depth.

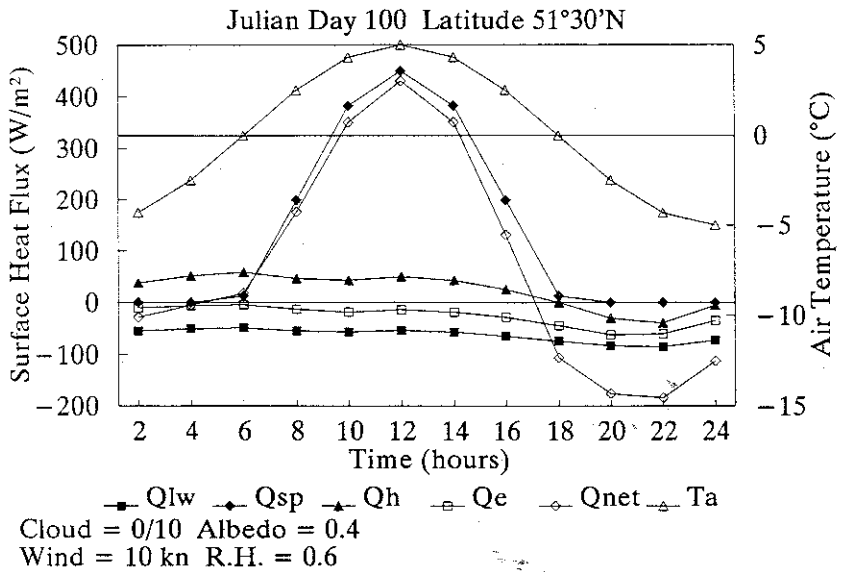
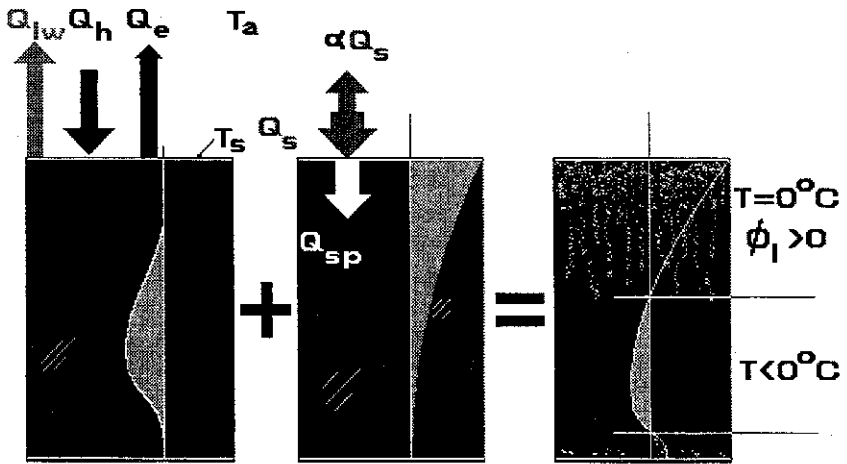


FIGURE 2 Schematic of heat-flux terms and meteorological conditions generated by ROT for CASE II-Surface Deterioration.



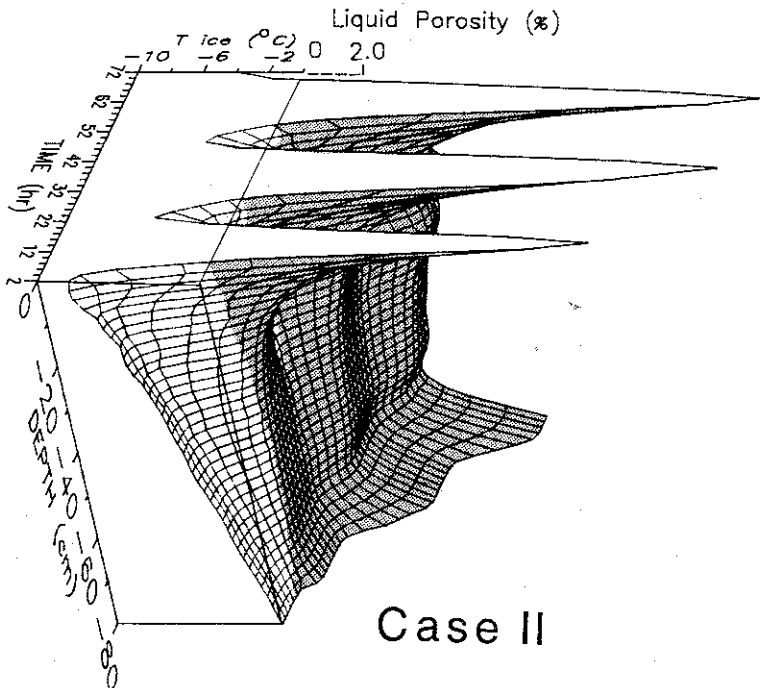
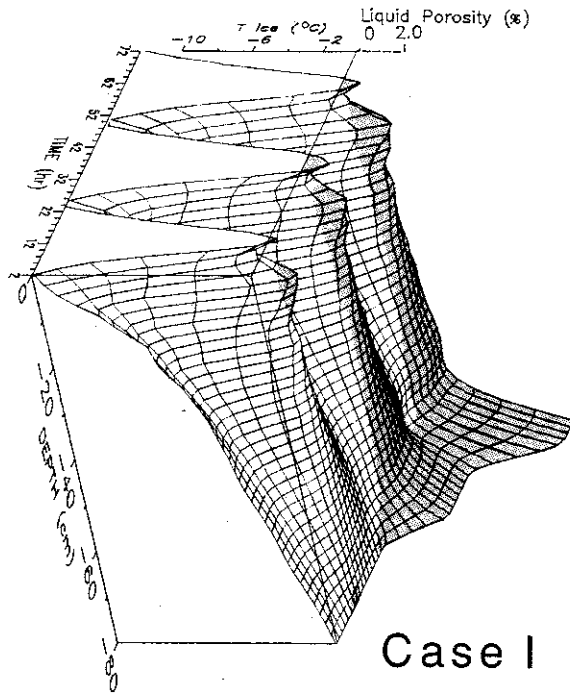


FIGURE 3 Time series of warming, nocturnal cooling and structural deterioration for three consecutive days under the influence of the meteorological conditions described in Figures 1, 2.

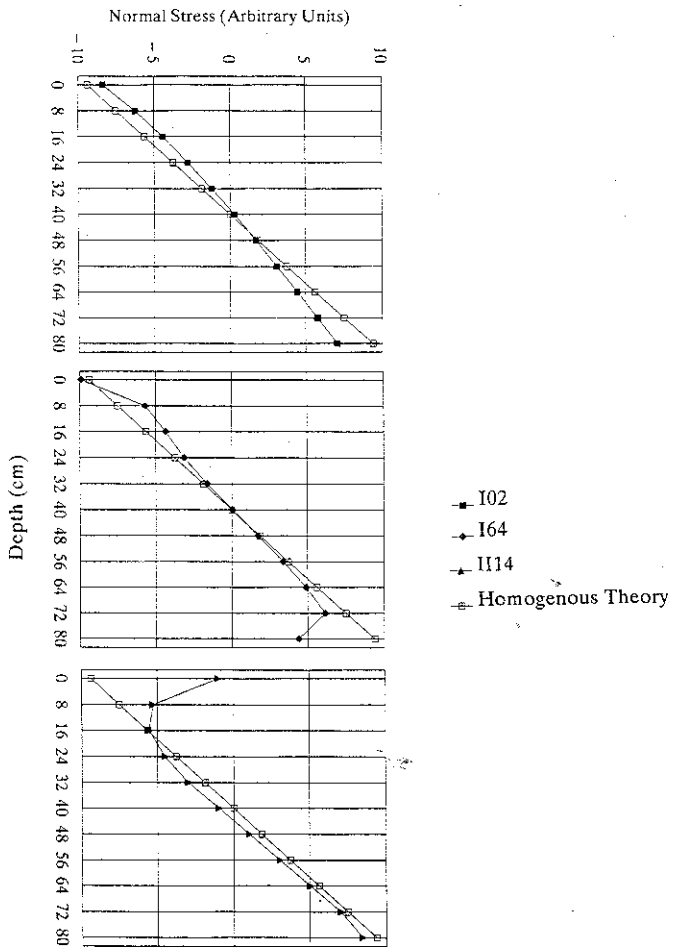
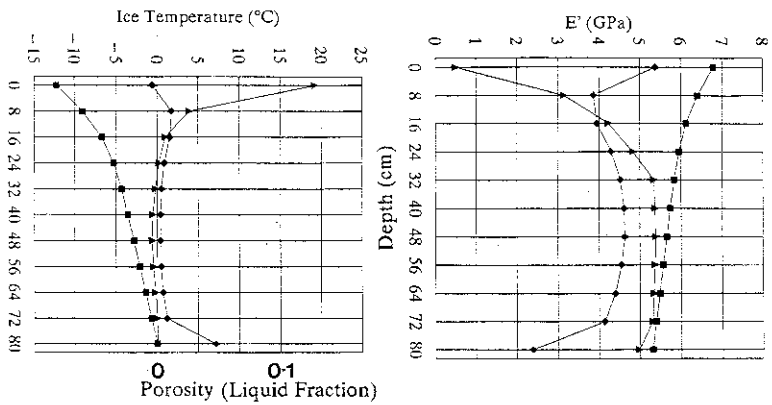


FIGURE 4 Extracted profiles of ice temperature, porosity, the resulting effective strain modulus distribution,  $E'(z)$  and the corresponding bending-stress distribution.